

Supporting Information

Enhancement of Oxygen Reduction Activities by Pt Nanoclusters Decorated on Ordered Mesoporous Porphyrinic Carbons

Sun-Mi Hwang^a, YongMan Choi^b, Min Gyu Kim^c, Young-Jun Sohn^a, Jae Yeong Cheon^d, Sang Hoon Joo^{d,e}, Sung-Dae Yim^a, Kurian A. Kuttiyiel^f, Kotaro Sasaki^f, Radoslav R. Adzic^f, and Gu-Gon Park^{a*}

*Corresponding Author: gugon@kier.re.kr

^aFuel Cell Laboratory, Korea Institute of Energy Research (KIER), Daejeon 305-343, South Korea

^bSABIC Technology Center, Riyadh 11551, Saudi Arabia

^cPohang Accelerator Laboratory, Pohang 790-784, Republic of Korea

^dDepartment of Chemistry, Ulsan National Institute of Science and Technology (UNIST), Ulsan 689-798, South Korea

^eSchool of Energy and Chemical Engineering, Ulsan National Institute of Science and Technology (UNIST), Ulsan 689-798, South Korea

^fChemistry Department, Brookhaven National Laboratory, Upton, New York 11973, USA

Figure Legends

Figure S1. Polarization curves for the ORR on FeCo-OMPC(L), OMPC(L), and Vulcan XC-72 (VC) in O₂-saturated 0.1 M HClO₄ with a sweep rate of 10 mV/s at 1600 rpm.

Figure S2. Normalized (a) Fe k-edge and (b) Co k-edge XANES spectra for FeCo-OMPC(L), 5% Pt/FeCo-OMPC(L), 10% Pt/FeCo-OMPC(L) catalysts, and CoTMPP, FeTMPPCl precursors.

Figure S3. The bulk structure of FeCo-OMPC(L) consisting of 152 atoms (120 C, 12 N, 14 O, 2 Fe, 2 Co, and 2 H).

Figure S4. (a) The surface model with the (0001) surface plane consisting of 152 atoms (120 C, 12 N, 14 O, 2 Fe, 2 Co, and 2 H). The Co metal on the topmost layer was replaced by Pt to explain the Pt nanocluster growth. and (b) schematic side view of the FeCo-OMPC(L) surface without the M defect.

Figure S5. Schematic of the growth of Pt nanocluster on FeCo-OMPC(L). M and V are a metal center and its vacancy, respectively.

Figure S6. Schematic illustration of the growth of Pt nanocluster on FeCo-OMPC(L) with (a) Pt₁, (b) Pt₆, and (c) Pt₁₉.

Figure S7. Specially designed *in situ* electrochemical cell for X-ray absorption spectroscopy (XAS) analysis.

Figure S1

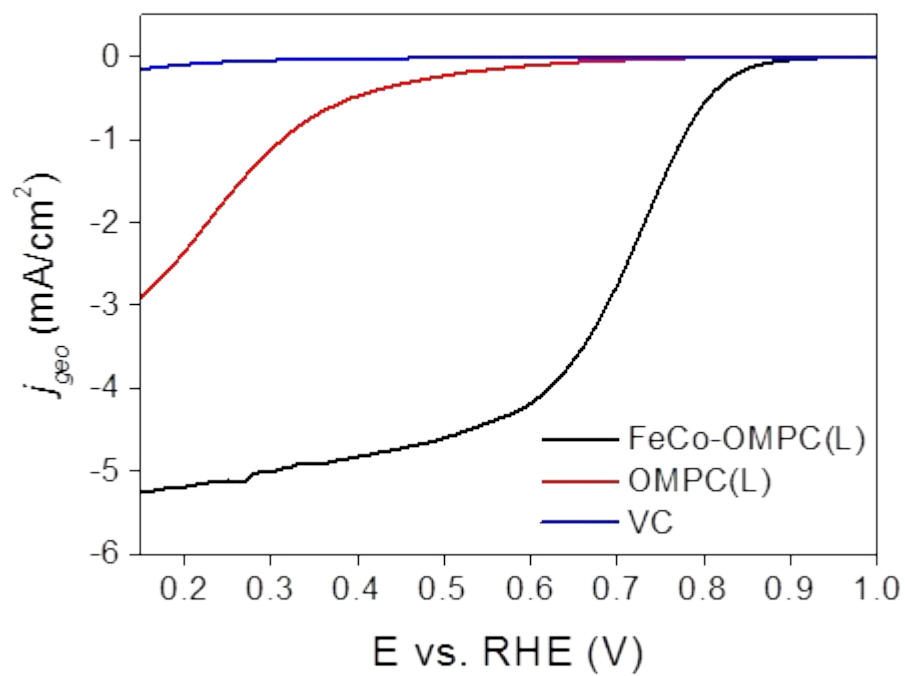


Figure S2

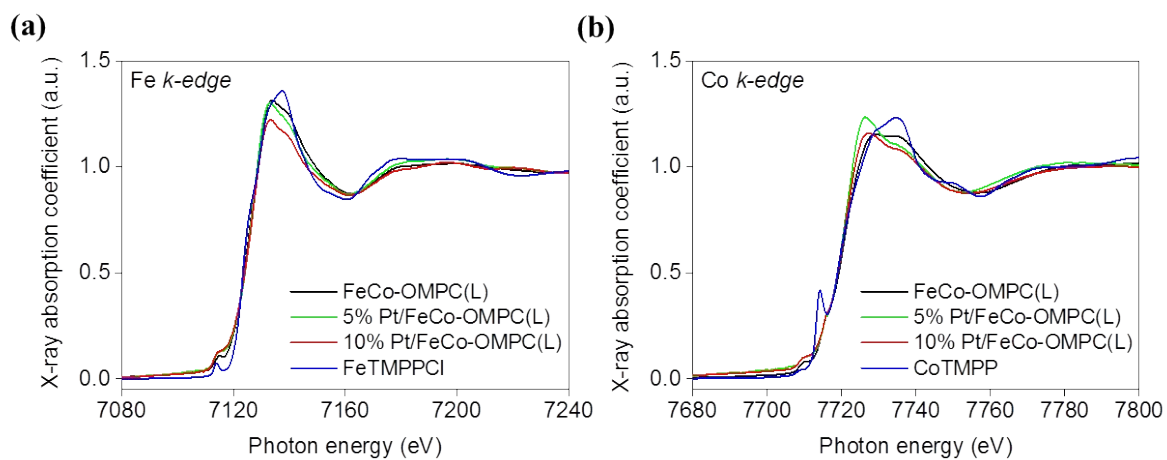


Figure S3

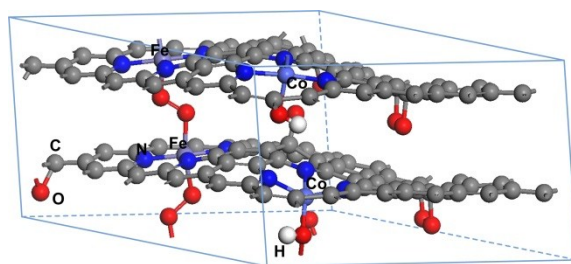


Figure S4

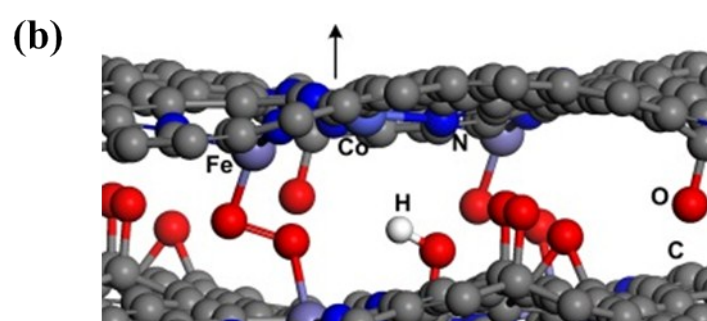
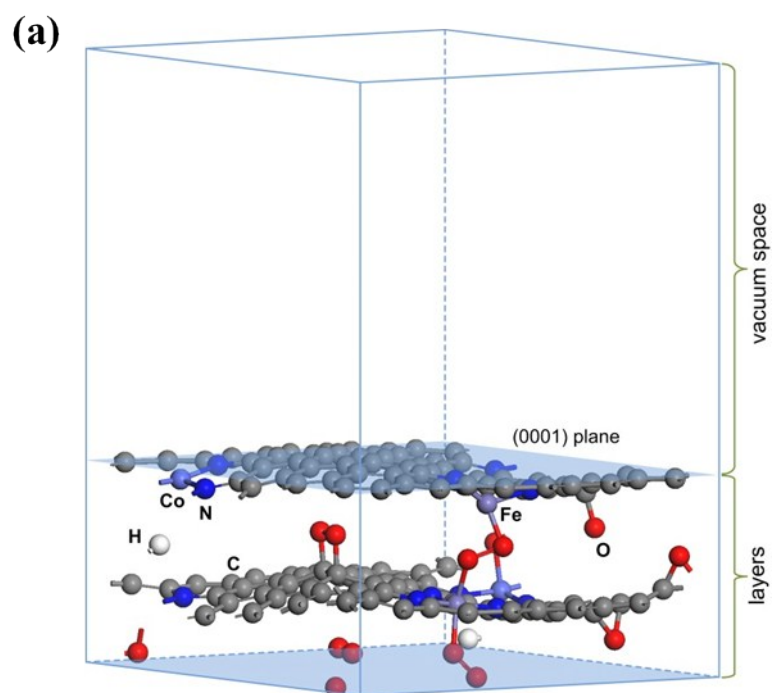


Figure S5

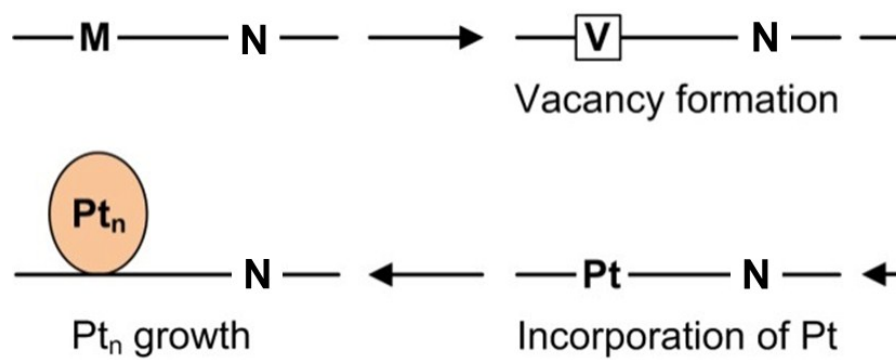


Figure S6

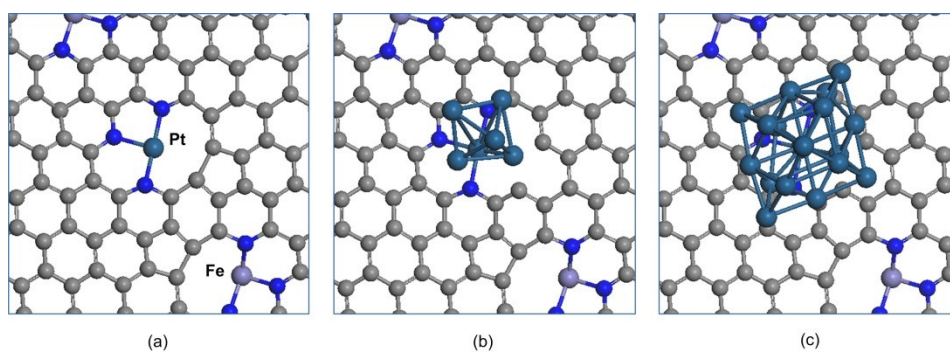


Figure S7

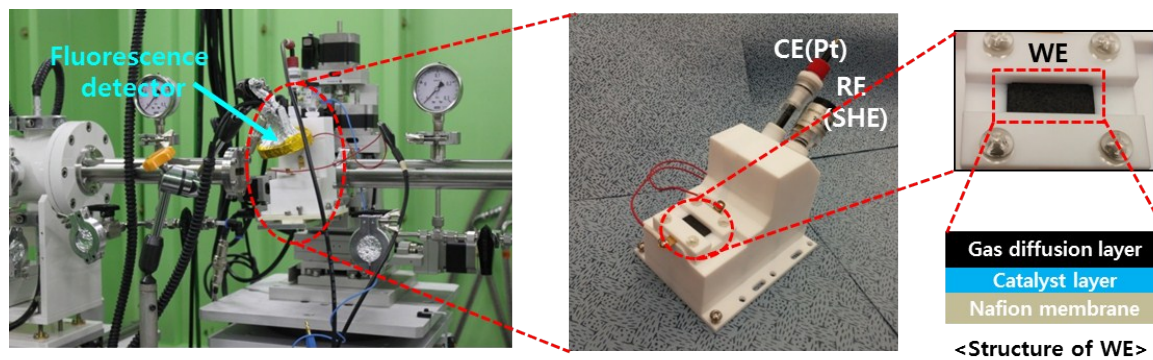


Table S1. Comparison of Pt particle size (d_{Pt}) calculated from XRD, and half-wave potentials ($E_{1/2}$), kinetic current density (j_k), specific activity (j_s), and mass activity (j_m) at 0.9 V vs. RHE, and ECSA measured by CO stripping of the prepared catalysts and commercial Pt/C

<i>Catalysts</i>	d_{Pt} (nm)	$E_{1/2}$ (mV)	j_k (mA/cm ²)	j_s (μ A/cm ²)	j_m (A/mg _{Pt})	<i>ECSA</i> (m ² /g _{Pt})
FeCo-OMPC(L)	-	723	0.15	-	-	-
3% Pt/FeCo-OMPC(L)*	4.5 \pm 2.5	782	0.06	26	0.03	96.85
5% Pt/FeCo-OMPC(L)*	2.1 \pm 0.7	858	1.33	350	0.30	84.81
10% Pt/FeCo-OMPC(L)*	2.3 \pm 0.6	866	1.65	258	0.25	96.45
5% Pt/OMPC(L)*	3.5 \pm 1.3	845	0.94	157	0.15	96.58
5% Pt/C*	6.8 \pm 0.8	755	0.16	50	0.04	80.50
Commercial Pt/C (JM)	3.2 \pm 0.3	894	5.33	344	0.16	46.83

*In here, we compared the catalytic activity with lower amount of Pt loading (ca. 3.8-4.5 μ g_{Pt}/cm²) than 20 μ g_{Pt}/cm² generally used for Pt/C evaluation to elucidate the effect of low Pt on FeCo-OMPC(L) relative to Pt supported on OMPC(L) or carbon.

Table S2. The vacancy formation energies for the metal centers and incorporation energies of Pt

	E_{M-vac} (eV/atom) ^a	$E_{Pt-incorp}$ (eV/atom) ^b
Co	6.09	-5.03
Co, Fe	6.34	-4.73
Fe	6.74	-4.80

a. Vacancy formation energy of M.

b. Incorporation energy of Pt atom into a metal vacancy.

Table S3. Coordination number and geometrical parameters calculated using DFT^a

<i>Surface</i>	<i>N</i>	$r_{(Co-N)} (\text{\AA})$	$r_{(Fe-N)} (\text{\AA})$	$r_{(Pt-N)} (\text{\AA})$	$r_{(Pt-Pt)} (\text{\AA})$
Bulk OMPC(L)	3	1.83	1.84	-	-
Pt ₁ /FeCo-OMPC(L) _{def}	3	1.83	1.87	1.93	-
Pt ₆ /FeCo-OMPC(L) _{def}	3	1.83	1.87	1.95	2.58
Pt ₁₉ /FeCo-OMPC(L) _{def}	3	1.83	1.87	1.97	2.64

a. FeCo-OMPC(L)_{def} is the surface with a Co vacancy on the topmost surface.